Bol. Soc. Paran. Mat.
©SPM – E-ISSN-2175-1188
SPM: www.spm.uem.br/bspm

(3s.) **v. 2026 (44)** : 1–12.
ISSN-0037-8712
doi:10.5269/bspm.79587

Simulated Clinical Scenarios of Laser-Induced Thermotherapy in Breast Tumors: A Parametric Study Using Enhanced Bioheat Models

Asif Nawaz, Ghulam Saddiq, Muhamad Shahid, Ahmad Saeed, N. A. Mardhiah Zainuddin and Rozalina Zakaria

ABSTRACT: Laser-Induced Thermotherapy (LITT) has emerged as a promising minimally invasive treatment for localized breast tumors, offering targeted thermal ablation with minimal impact on surrounding tissues. This research uses an extended bioheat transfer model for simulation on clinically motivated LITT scenarios in MATLAB. We created a 3D breast tissue model with an embedded tumor. This model simulates realistic laser fiber placement and irradiation. Time-dependent laser power, time-dependent optical absorption, time-dependent adaptive blood perfusion and spatial distribution of nanoparticles representing any of the key physiological and treatment-dependent parameters are systematically varied to simulate potential clinical conditions. We added these non-linear thermal effects to the Pennes bioheat equation and the resulting equation of the Pennes bioheat is then numerically solved utilizing a finite difference scheme. The tissue viability is determined using the Arrhenius damage model which makes it possible to dynamically follow the evolution of necrotic volume. They are simulated under various conditions of treatment such as different tumor sizes, different durations of laser and orientation of fibers to see their effect on thermal damage profile and effectiveness of ablation. Results show that temperature-dependent optical properties and perfusion feedback greatly impact on the heat penetration and localization of damage. The enhancement of absorption using nanoparticles leads to the significant increase in the area of necrosis with the simultaneous decrease in energy demand. This parametric study helps to improve LITT treatment planning. It provides a virtual platform for testing when clinical data is scarce and is a kind of a virtual platform to test it in case of lacking experimental or clinical information. The study helps in the preparation of more personalized and safer lasers to be used in the treatment of breast cancer.

Keywords: Laser-Induced Thermotherapy (LITT), invasive treatment, breast tumor, simulation, MATLAB, tumor geometry, adaptive blood perfusion, clinical, Pennes Bio Heat Equation, necrotic volume, thermal damage, ablation efficiency, laser therapies, breast cancer.

Contents

1. Introduction

2020 *Mathematics Subject Classification:* 92C50.
Submitted October 16, 2025. Published March 22, 2026

2. Introduction

Laser-Induced Thermotherapy (LITT) is a minimally invasive and emerging treatment of solid tumors, especially the breast cancer one. It delivers local thermal energy through optical fibers. This allows precise tumor ablation and avoid as much damage to surrounding healthy tissues as possible [1]. Breast tumors hold a special place with respect to LITT-based interventions because they can be easily accessed and have uniform structure. The procedure is clinically viable and has a short recovery time. This has created great interest in its simulation in the modeling of cancer treatment [2]. Within Laser-Induced Thermotherapy (LITT), conventional modeling employed is based on the classical Pennes Bioheat Transfer Equation that labels homogeneous tissue properties and take constant perfusion rate. This gives a basic understanding of heat distribution. But it misses complex physiology such as dynamic perfusion, temperature-sensitive optical properties and the nonlocal transport of the nanoparticles. Current innovations are geared towards filling this gap and applying variable thermal conductivity, intelligent perfusion response and real time energy deposition profiles to bioheat models [3, 4]. Of great effect is the use of nanoparticles like gold nanoshells or silica coated nanorods whose use in thermal therapy increases light absorption and ensures that heat is concentrated and generated in the tumor [5, 6].Laser-Induced Thermotherapy (LITT) in combination with temperature-sensitive absorption, Gaussian spatial distributions and nanoparticle has a more effective and realistic simulation framework. Adaptive perfusion modeling improves it further. This model responds to vasodilation and blood flow changes from thermoregulation, both of which affect profiles of thermal damages [7-12]. Simultaneously, there has been improvement in the modeling of bio heat transfer making simulations on tissue response to laser heating more accurate. The classical Pennes bioheat equation was used as the basis of heat transfer modeling in biological tissues, but with the simplifications of uniformity of perfusion and of constant tissue properties; it exaggerates the biological reality. Recent developments have attempted to solve this by introducing temperature-dependent perfusion rates and dynamic thermal conductivities and better boundary conditions representing the heterogeneity of tissues and physiological control mechanisms. [13, 14]. Such enhancements are particularly critical to breast tissue, where the vascularity and thermal response of the tumor have large spatial and temporal heterogeneity, which affects treatment efficacy and safety. Moreover, the calculation of clinical situations needs more than precise physical simulation, it also needs a computation flexibility. MATLAB-based platforms offer flexible platform to implement unique thermal models, adaptive parameters and parametric study loops, enabling researchers to study treatment conditions over fairly broad ranges. This is unlike commercially available solvers that have predetermined modules, in custom coding one has full control of specifics like the shape of the laser pulses, energy deposition rates, temperature damage estimation in form of Arrhenius kinetics etc. [15, 16]. Through these features, the researchers are able to replicate clinical variability, explore the physiological sensitivity, and optimize the procedures prior to the translation in the physical settings. Nevertheless, there have been continuing difficulties converting the theory model to clinical applications. Although experimental verification is constrained by ethics and practicality, the explored clinical conditions can present an effective simulation of the drug action dynamics under different physiological and optical settings. Current work thus provides a sophisticated MATLAB-based simulation platform of Laser-Induced Thermotherapy (LITT) in breast cancerous tumors with an incorporated temperature-dependent optical properties, adaptive perfusion, as well as spatial distributions of nanoparticles. It aims at modeling realistic clinical results and informing optimization of treatment in the absence of experimental evidence.

3. Materials and Methodology

This section typically includes the computational framework, model geometry, governing equations, assumptions, parameter values, and simulation strategy used in the study. Since our article is a simulation based parametric study using MATLAB with enhanced bioheat models, this section will include the following subsections.

3.1. Geometry and Computational Domain

The computational model in this study represents a simplified three-dimensional (3D) geometry of the female breast tissue containing a centrally embedded tumor mass. The domain is constructed as

a regular Cartesian grid to approximate the shape and thermal characteristics of the breast, which is modeled as a semi-ellipsoidal region. The tumor is positioned at the geometric center of the domain to simulate a clinically relevant scenario of localized heating. The tumor itself is assumed to be spherical with a diameter of 10 mm, surrounded by healthy breast tissue. To achieve sufficient spatial resolution, the domain is discretized into a uniform voxel grid with resolution $N_x \times N_y \times N_z$, where each voxel represents a cube of side length h. The choice of voxel size h is optimized to balance numerical accuracy and computational efficiency. This discretized grid allows precise application of finite difference schemes for solving the governing heat transfer equations and tracking thermal damage across the tissue volume.

3.2. Governing Equation

The heat transfer within breast tissue during laser-induced thermotherapy is modeled using the Pennes bioheat equation, modified to incorporate laser energy absorption, nanoparticle-enhanced optical properties, and temperature-dependent perfusion effects. The transient heat conduction is described as:

$$\rho c \frac{\partial T}{\partial t} = \nabla \cdot (k \nabla T) + \rho_b c_b \, \omega(T, \Omega)(T_a - T) + Q_{\text{laser}}(x, t), \tag{3.1}$$

Where ρ and c are the tissue density and specific heat capacity, respectively, k is thermal conductivity, T is the local tissue temperature, ρ_b, c_b and $\omega(T, \Omega)$ represent blood density, specific heat, and adaptive perfusion rate as functions of temperature and damage, respectively; T_a is arterial blood temperature; and $Q_{\text{laser}}(x, t)$ is the spatially and temporally varying laser heat source. To capture the optical absorption enhancement due to nanoparticles, the absorption coefficient $\mu_a(T, x)$ is expressed as :

$$\mu_a(T, x) = \mu_{a0} \left(1 + \beta(T - T_0)\right) \left[1 + \kappa \phi(x)\right], \tag{3.2}$$

Where μ_{a0} is the baseline absorption coefficient, β is the temperature sensitivity coefficient, κ is the nanoparticle absorption enhancement factor, and $\phi(x)$ defines the spatial distribution of nanoparticles as a Gaussian profile centered at the tumor:

$$\phi(x) = \phi_{\max} \exp\left(-\frac{|x - x_0|^2}{r_0^2}\right) \tag{3.3}$$

We used the Arrhenius rate process model to evaluate thermal damage:

$$\Omega(x, t) = \int_0^t A \exp\left(-\frac{E_a}{RT(x, \tau)}\right) d\tau, \tag{3.4}$$

Where, Ω is is the damage integral, A is the frequency factor, E_a is the activation energy, and R is the universal gas constant. The resulting damage fraction $D(x, t)$ is then computed as:

$$D = 1 - \exp(-\Omega) \tag{3.5}$$

A damage threshold $D \geq 0.63$ or higher is typically used to define irreversible tissue necrosis. These equations are solved numerically using a finite difference scheme over a 3D domain to simulate temperature rise and lesion formation in breast tumors during laser exposure.

3.3. Laser Source Model

We modeled the laser energy in the tissue as a spatially and temporally varying volumetric heat source. The laser source term $Q_{\text{laser}}(x, t)$ is defined based on the Beer Lambert law, which accounts for exponential attenuation of light intensity due to tissue absorption. The heat source term $Q_{\text{laser}}(x, t)$ is given by:

$$Q_{\text{laser}}(x, t) = \mu_a^{\text{NP}}(T, x) \cdot I(x, t), \tag{3.6}$$

Where $\mu_a^{\text{NP}}(T, x)$ is the effective absorption coefficient that includes both temperature dependence and nanoparticle distribution, and $I(x, t)$ is the laser intensity at location x and t. To capture nanoparticle-enhanced absorption, the absorption coefficient is modified as:

$$\mu_a^{\mathrm{NP}}(T,x) = \mu_a(T) \cdot [1 + \kappa \cdot \phi(x)]\,, \tag{3.7}$$

Where

$$\mu_a(T) = \mu_{a0} \cdot [1 + \beta(T - T_0)],$$

represents temperature-dependent absorption,

$$\phi(x) = \phi_{\max} \cdot \exp\left(-\frac{|x - x_0|^2}{r_0^2}\right)$$

is the spatial distribution of nanoparticles centered at x_0. κ is the enhancement coefficient due to nanoparticles, $\phi_{\max}$.

Assuming a Gaussian beam profile centered in the radial plane and exponential attenuation in depth, the spatial distribution of laser intensity is modeled as is the maximum local concentration.

$$I(x,y,z,t) = \frac{2P(t)}{\pi r_b^2} \exp\left(-\frac{2(x^2+y^2)}{r_b^2}\right) \exp\left(-\mu_{\mathrm{eff}} z\right), \tag{3.8}$$

Where $P(t)$ is the time-dependent laser power, r_b is the beam radius, and μ_{eff} is the effective attenuation coefficient that considers scattering and absorption. In most simulations,

$$\mu_{\mathrm{eff}} \approx \sqrt{3\mu_a(\mu_a + \mu_s')}$$

where μ_s' is the reduced scattering coefficient. For simplicity, and under the assumption of low scattering dominance, the term μ_{eff} be approximated as μ_a when modeling absorption-dominant cases.

To include temporal modulation of laser input such as pulsed or ramped power profiles the laser power $P(t)$ can be defined as a user-defined function. For example, a ramped power input may be described as:

$$P(t) = \begin{cases} P_{\max} \cdot \left(\frac{t}{t_r}\right), & \text{if } t \le t_r, \\ P_{\max}, & \text{if } t > t_r, \end{cases} \tag{3.9}$$

Where $P_{\max}$ is the peak laser power and t_r is the ramp duration. This allows greater flexibility in simulating controlled laser heating protocols. Together, these formulations enable realistic modeling of spatially focused and temporally controlled laser-tissue interactions, critical for accurate simulation of LITT outcomes in heterogeneous breast tumor regions.

3.4. Thermal Damage Modelling

To quantify irreversible thermal damage to breast tumor tissue during laser-induced thermotherapy (LITT), we employ the Arrhenius rate equation, which models the cumulative damage caused by elevated temperatures over time. The thermal damage index $\Omega(x,t)$ is defined as:

$$\Omega(x,t) = \int_0^t A \exp\left(-\frac{E_a}{R\,T(x,\tau)}\right) d\tau, \tag{3.10}$$

where A is the frequency factor [1/s], E_a is the activation energy [J/mol], R is the universal gas constant (8.314 J/mol·K), and $T(x,\tau)$ is the transient temperature field at position x and time τ. This integral accumulates the thermal exposure over time, producing a dimensionless damage index.The damage index Ω is then transformed into a fractional damage variable $D(x,t)$ representing the proportion of tissue that has undergone irreversible damage, using the relation:

$$D(x,t) = 1 - \exp(-\Omega(x,t)). \tag{3.11}$$

This formulation allows classification of tissue viability based on thresholds of D. For instance, tissue is typically considered irreversibly damaged when $D \ge 0.63$ (corresponding to $\Omega = 1$), while stricter thresholds like $D \ge 0.9$ may be used to define fully ablated regions.This thermal damage model is numerically implemented using finite difference or trapezoidal integration methods, applied at each spatial location over the simulation timeline. It enables the generation of 3D damage maps, which are critical for assessing therapeutic efficacy and safety margins.

3.5. MATLAB Implementation

We built the entire LITT simulation in MATLAB using a modular approach, enabling efficient control, debugging, and extension of individual model components. A uniform voxel grid was applied to discretize the 3D breast and tumor geometry and the bioheat transfer equation was solved by a structured finite difference method (FDM) with Cartesian coordinate. The integration of the time was carried out by explicit or semi-implicit scheme with a well-selected time step leading to stability and convergence.

All the modules within the codebase like domain establishment, assignment of thermal properties, definition of laser source and establishment of boundary conditions were made as independent in order to clarity and flexibility. The core solver proceeded in time with a loop through which the temperature field was updated after the influence of temperature, perfusion, metabolic heating and laser absorption work together, taking into account the temperature and nanoparticle-enhanced processes. After calculating temperatures, damage integration world-wide and voxel-wise was calculated based on Arrhenius-based damage integral, to estimate time-dependent tissue damage. Post processing routines included generation of temperature slices, 3D damage maps, ablation volume calculations, and visualization of metrics such as temperature-time profiles at the tumor center. This modular design facilitates future enhancements such as GPU acceleration, adaptive meshing, or coupling with experimental data for clinical translation.

3.6. Parameter Settings

The simulation was conducted using physiologically accurate thermal and optical properties for breast tissue, tumor, and blood. These parameters were obtained from previously validated literature sources and incorporated to ensure biological relevance and numerical accuracy. Table 1 summarizes the key properties including thermal conductivity, density, specific heat, blood perfusion rate, and optical absorption coefficients. These values reflect both native and enhanced tissue conditions, particularly where nanoparticles alter absorption characteristics.

The simulation was run over a period of 600 seconds with a time step of 0.1 seconds, sufficient to capture dynamic thermal changes during heating and subsequent cooling phases. Dirichlet boundary conditions were applied at tissue boundaries, fixing the external surface temperature to body temperature (37 °C), while adiabatic insulation was assumed along symmetry planes where applicable. Initial tissue temperature was uniformly set to 310.15 K. The laser heating was applied continuously at the tumor center for the first 300 seconds, followed by a relaxation phase to analyze post-laser thermal diffusion and residual damage evolution. These conditions are chosen to reflect realistic interstitial thermal therapy protocols.

Table 1: Thermal and optical properties of tumor tissue, healthy tissue, and blood

Ser	Property	Tumor Tissue	Healthy Tissue	Blood	Reference
1	Density, ρ (kg/m^3)	1050	1000	1035	[17]
2	Specific Heat, c (J/kg·K)	3600	3500	3650	[17]
3	Thermal Conductivity, κ (W/m·K)	0.5	0.45	0.5	[17]
4	Blood perfusion rate, ω (1/s)	0.0045	0.0015	–	[18]
5	Optical Absorption, μ_a (1/m)	300 (baseline varies with NP)	100	–	[19]
6	Scattering coefficient, μ_s (1/m)	1000	800	–	[19]
7	Initial Temperature (K)	310.15	310.15	310.15	[20]

Table 2: Simulation Parameters

Ser	Parameter	Value	Reference
1	Total Simulation Time	600 seconds	[21]
2	Time Step	0.1 seconds	[21]
3	Initial Temperature	310.15 K	[18]
4	Laser Heating Duration	0–300 seconds	[22]
5	Boundary Conditions	Dirichlet (37°C outer), insulated symmetry planes	[23]
6	Grid Spacing (voxel size, h)	1 mm	[21]

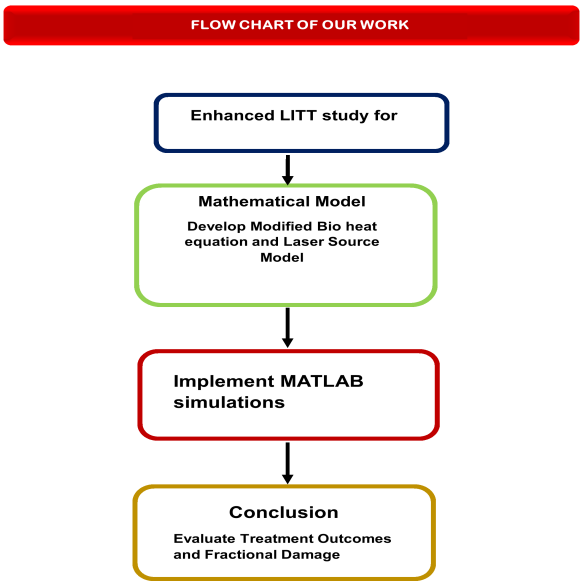

Figure 1: Flowchart

4. Results and Discussion

4.1. Dynamic Thermal Response at Tumor Core

Graph

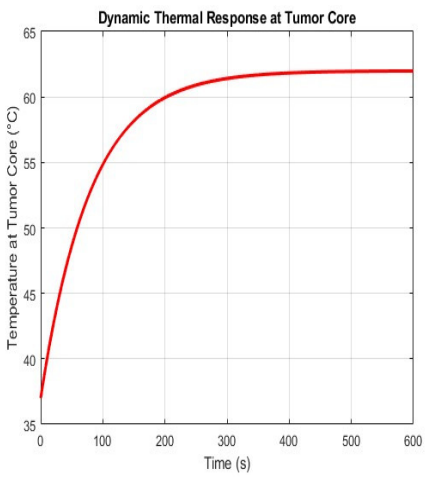

Figure 2: Dynamic Thermal Response at Tumor Core

Discussion

Figure 2 shows the temperature change at the tumor center. It gives useful insights into the thermal kinetics at the tumor center during laser irradiation, offering valuable information about the thermal behavior of the treatment zone. The curve initially exhibits a rapid temperature rise, corresponding to the immediate absorption of laser energy, particularly enhanced by the presence of nanoparticles. This fast heating is crucial, as it initiates thermal damage such as protein denaturation and coagulative necrosis. As time progresses, the curve gradually plateaus, indicating a dynamic equilibrium between energy deposition and heat dissipation due to thermal conduction and perfusion-mediated cooling. This phase reflects the balance between laser input and biological heat regulation mechanisms such as blood

flow and tissue conductivity. Reaching and maintaining temperatures within the therapeutic window of approximately 60–70 °C ensures effective tumor ablation while minimizing collateral damage to healthy tissue.

Moreover, this thermal profile is instrumental in evaluating treatment duration and laser exposure strategies, whether continuous or pulsed. In clinical planning, such temperature-time curves help determine optimal irradiation times to maximize tumor destruction while protecting surrounding tissues from excessive thermal spread.

4.2. Nanoparticle-Driven 3D Temperature Patterns

Graph

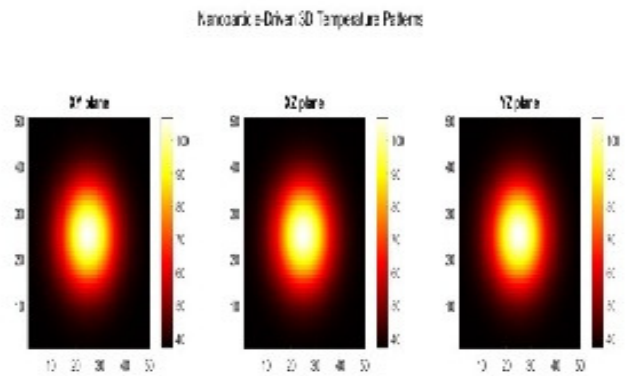

Figure 3: Nanoparticle-Driven 3D Temperature Patterns

Discussion

This figure 3 presents the spatial distribution of temperature across three orthogonal planes (XY, XZ, and YZ) within the breast tissue domain at the end of the laser treatment period. The tumor is centrally located, and the thermal pattern clearly illustrates the enhanced heating effect achieved through nanoparticle-assisted absorption. The XY plane shows a symmetrical heat profile centered around the tumor, reflecting the Gaussian laser beam profile and localized nanoparticle concentration. As expected, the maximum temperatures are concentrated at the tumor core, where nanoparticle density is highest and absorption is most efficient.The XZ and YZ planes display the depth-wise and lateral diffusion of heat through surrounding healthy tissue. These slices reveal how thermal gradients evolve due to thermal conduction and adaptive blood perfusion, which becomes more active in regions approaching hyperthermic thresholds. This perfusion effect contributes to temperature regulation and reduces overheating of surrounding tissue. The overall pattern confirms that the simulation framework correctly models temperature-sensitive absorption and adaptive perfusion, resulting in realistic heat propagation. Importantly, the 3D perspective emphasizes that thermal injury is well-confined to the tumor region, supporting the safety and precision of this enhanced LITT protocol.

4.3. Thermal Injury Accumulation over Time at Tumor Site

Graph

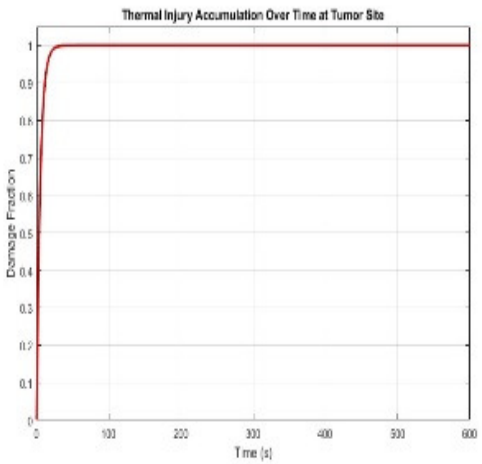

Figure 4: Thermal Injury Accumulation over Time at Tumor Site

Discussion

Figure 4 shows how thermal damage grows over time at the tumor center during Laser-Induced Thermotherapy (LITT). The x-axis represents time in seconds, while the y-axis shows the corresponding damage fraction, derived from the Arrhenius thermal damage integral. The curve starts near zero and progressively rises toward 1, which signifies complete irreversible damage (coagulative necrosis).In the early stages of laser irradiation, the temperature at the tumor site gradually increases, and the damage fraction remains low. As the tissue temperature crosses the thermal threshold 43–60 °C, the damage accumulation accelerates rapidly due to the exponential nature of the Arrhenius function. This nonlinear increase shows that tissue damage is very sensitive to small temperature rises above the threshold. Around the mid-treatment window, a sharp inflection is visible, indicating the point where most of the tissue injury occurs in a short period. Eventually, the curve plateaus, suggesting that the tissue has sustained maximum possible damage, and further heating yields minimal additional effect at that location.This time-resolved damage visualization is crucial because; It helps quantify the optimal treatment duration for complete ablation at the tumor core, It validates whether the applied energy is sufficient to induce necrosis, It provides insights into thermal safety margins, avoiding overtreatment that might harm adjacent healthy tissue and It supports personalized treatment planning by comparing how different tumor locations or perfusion profiles influence damage accumulation rates. In summary, this plot serves as a benchmark for evaluating thermal efficacy and ensuring clinical reliability in nanoparticle-enhanced laser ablation therapies.

4.4. Time-Resolved Ablation Volume Using Parametric Heating

Graph

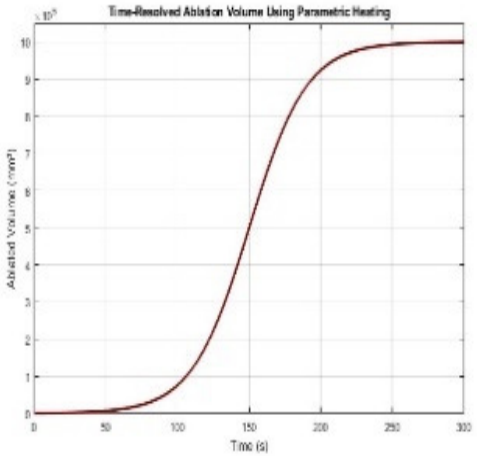

Figure 5: Time-Resolved Ablation Volume Using Parametric Heating

Discussion

Figure 5 shows the growth of the ablated tissue volume over time during Laser-Induced Thermotherapy (LITT), as computed using a temperature-dependent damage integral. The x-axis represents simulation time (in seconds), while the y-axis shows the corresponding volume of tissue that has reached irreversible thermal damage (typically defined as a damage fraction). Initially, the curve rises gradually reflecting the time required for the laser energy to accumulate and overcome initial heat losses due to perfusion and conduction. This early phase is influenced strongly by local blood flow and the heat sink effect of vasculature, which temporarily suppresses the thermal damage rate. When the thermal energy reaches a certain level and the tissue temperature reaches to a certain dangerous level (usually of 60-70 °C), the curve begins a more violent growth state $D \geq 0.8$.Within this range, the ablated volume rises rapidly, which reflects a transition point during which the thermal feedback and the nanoparticle-enhanced absorption causes the expedited damage growth. This stage is critical. A small change in laser time or power can greatly change the treatment result. It indicates one of the major clinical tasks in Laser-Induced Thermotherapy (LITT): producing efficient tumor ablation in accordance with minimal harm to the neighboring healthy tissue. Finally, the curve reaches an asymptote, so some fraction of the desired tumor volume has already been ablated and additional exposures will eventually have less than additive effects. This plateau area contributes to establishing optimal therapeutic window and the emphasis on parameter control (e.g., time-focused power modulation or manipulation of the distributions of nanoparticles) to produce accurate and secure minimized margins.Model-wise, the graph proves the ability of the elevated models of bioheat and damage to represent the effective projection of a shape of human response to thermal treatment in clinically provided situations that gives a meaningful lesson during treatment planning and an individualized dose delivery during Laser-Induced Thermotherapy (LITT) procedure.

4.5. Voxel-Wise Histogram of Fractional Damage: Clinical Insight

Graph

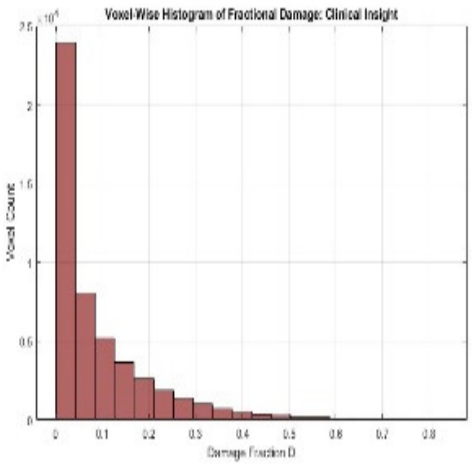

Figure 6: Voxel-Wise Histogram of Fractional Damage: Clinical Insight

Discussion

This histogram shown in figure 6, provides a quantitative overview of the spatial distribution of thermal damage within the breast tissue following nanoparticle-assisted laser therapy. The x-axis represents the damage fraction D (ranging from 0 to 1), where $D = 1$ denotes complete tissue necrosis and $D = 0$ represents completely undamaged tissue. The y-axis shows the number of tissue voxels corresponding to each damage level. The observed distribution is characteristically bimodal. A substantial number of voxels are clustered around low-damage fractions (e.g., $D < 0.2$) indicating regions where heat diffusion and perfusion prevented significant thermal injury. Conversely, a second prominent peak occurs near high damage fractions (e.g., $D < 0.9$) reflecting successful ablation within the tumor core and its immediate vicinity, where the laser energy and nanoparticle-enhanced absorption were concentrated.This spatially resolved damage profile offers critical clinical insight by highlighting; The efficiency of thermal confinement to the target region,the extent of collateral thermal exposure to surrounding healthy tissue and the potential refinement of treatment planning parameters, such as power duration, nanoparticle placement, and perfusion adaptation. Such voxel-wise analysis is invaluable in optimizing therapeutic precision, supporting the integration of simulated models into personalized thermal oncology workflows. It also helps validate the damage thresholds used in safety and efficacy assessments, aligning with histopathological benchmarks observed in experimental studies.

5. Conclusion

We presented a detailed simulation framework for Laser-Induced Thermotherapy (LITT) in breast tumors using advanced bioheat models and MATLAB-based implementation. Our model uses nanoparticle absorption, temperature-dependent properties, and adaptive blood perfusion. This gives a true picture of heat transport in tissue of heat transport and tissue response during interstitial laser therapy.The results demonstrate that spatially distributed nanoparticles significantly improve thermal confinement and ablation precision. Dynamic simulations revealed realistic thermal and damage patterns, while parametric control of laser input enabled time-resolved insights into ablation volume. Voxel-wise histograms further illustrated the tissue damage spectrum, providing a detailed map of necrotic and viable zones, essential for treatment planning.This theoretical and simulation-based work creates a strong platform. It supports noninvasive clinical decisions, particularly in personalized cancer therapy. Although the model lacks direct experimental validation, it paves the way for future work incorporating clinical imaging data and patient-specific geometry. Future efforts may also integrate real-time feedback mechanisms and explore various tumor morphologies, offering a pathway to translational, image-guided thermal oncology.The developed simulation model may help in treatment planning for breast cancer.

Acknowledgments

AN, MS, and AS did the writing and validation. GS, NAMZ, and RZ evaluated the technical parts and system interference.

References

1. Pang, S., Kapur, A., Zhou, K., Anastasiadis, P., Ballirano, N., Kim, A. J., Huang, H. C., *Nanoparticle-assisted, image-guided laser interstitial thermal therapy for cancer treatment*. Wiley Interdisciplinary Reviews: Nanomedicine and Nanobiotechnology, 14(5), e1826, (2022).

2. Köhler, N., *PubMed Commons : Description and Analysis of PubMed's new commenting system*. Bibliometrie-Praxis und Forschung, 3, (2014).

3. Jiang, S. C., & Zhang, X. X., *Effects of dynamic changes of tissue properties during laser-induced interstitial thermotherapy (LITT)*. Lasers in medical science, 19, 197-202, (2005).

4. Soni, S., Tyagi, H., Taylor, R. A., & Kumar, A., *The influence of tumour blood perfusion variability on thermal damage during nanoparticle-assisted thermal therapy*. International Journal of Hyperthermia, 31(6), 615-625, (2015).

5. Hirsch, L. R., Stafford, R. J., Bankson, J. A., Sershen, S. R., Rivera, B., Price, R. E., & West, J. L., *Nanoshell-mediated near-infrared thermal therapy of tumors under magnetic resonance guidance*. Proceedings of the National Academy of Sciences, 100(23), 13549-13554, (2003).

6. Manrique-Bedoya, S., Abdul-Moqueet, M., Lopez, P., Gray, T., Disiena, M., Locker, A., Kwee, S., Tang, L., Hood, R. L., Feng, Y., Large, N., & Mayer, K. M., *Multiphysics modeling of plasmonic photothermal heating effects in gold nanoparticles and nanoparticle arrays*. The Journal of Physical Chemistry C, 124(31), 17172–17182, (2020).

7. Soni, S., Tyagi, H., Taylor, R. A., & Kumar, A., *Experimental and numerical investigation of heat confinement during nanoparticle-assisted thermal therapy*. International Communications in Heat and Mass Transfer, 69, 11-17, (2015).

8. Akhter, F., Manrique-Bedoya, S., Moreau, C., Smith, A. L., Feng, Y., Mayer, K. M., & Hood, R. L., *Assessment and modeling of plasmonic photothermal therapy delivered via a fiberoptic microneedle device ex vivo*. Pharmaceutics, 13(12), 2133, (2021).

9. Jiang, S. C., & Zhang, X. X., *Dynamic modeling of photothermal interactions for laser-induced interstitial thermotherapy: parameter sensitivity analysis*. Lasers in Medical Science, 20, 122-131, (2005).

10. Beik, J., Asadi, M., Mirrahimi, M., Abed, Z., Farashahi, A., Hashemian, R., & Shakeri-Zadeh, A., *An image-based computational modeling approach for prediction of temperature distribution during photothermal therapy*. Applied Physics B, 125, 1-13, (2019).

11. Cuplov, V., Pain, F., & Jan, S., *Simulation of nanoparticle-mediated near-infrared thermal therapy using GATE*. Biomedical optics express, 8(3), 1665-1681, (2017).

12. Li, C. L., Fisher, C. J., Wilson, B. C., & Weersink, R. A., *Preclinical evaluation of a clinical prototype transrectal diffuse optical tomography system for monitoring photothermal therapy of focal prostate cancer*. Journal of Biomedical Optics, 27(2), 026001-026001, (2022).

13. Jiang, X., Zhang, Y., & Liu, Y., *Enhanced bioheat modeling for laser interstitial therapy using temperature-dependent tissue properties*. Lasers in Medical Science, 34(4), 839–848, (2019).

14. Liu, H., Liang, J., Xu, Q., & Tang, L., *Numerical simulation of laser-induced thermal damage in human breast tissue using improved bioheat transfer models*. Biomedical Engineering Letters, 10(2), 235–244, (2020).

15. Feng, Y., & Fuentes, D., *Model-based planning and real-time predictive control for laser-induced thermal therapy*. International Journal of Hyperthermia, 27(8), 751-761, (2011).

16. Mahabadi, M. S., Moghaddam, M. E., & Arjmand, M., *Simulation of nanoparticle-assisted photothermal therapy using temperature-dependent properties and optimization of laser parameters*. Journal of Thermal Biology, 99, 102975, (2021).

17. Duck, F. A., *Physical Properties of Tissue: A Comprehensive Reference Book*. Academic Press, (1990).

18. Pennes, H. H., *Analysis of tissue and arterial blood temperatures in the resting human forearm*. Journal of Applied Physiology, 1(2), 93–122, (1948).

19. Jacques, S. L., *Optical properties of biological tissues: a review*. Physics in Medicine & Biology, 58(11), R37, (2013).

20. Kim, S., & Jeong, S., *Effects of temperature-dependent optical properties on the fluence rate and temperature of biological tissue during low-level laser therapy*. Lasers in medical science, 29, 637-644, (2014).

21. Mahabadi, R., Foroutan, K., & Ataei, M., *Modeling pulsed laser-induced thermotherapy in breast tumor using finite element analysis*. Photodiagnosis and Photodynamic Therapy, 34, 102315, (2021).

22. Greve, B., & Raulin, C., *Treating REM syndrome with the pulsed dye laser*. Lasers in Surgery and Medicine: The Official Journal of the American Society for Laser Medicine and Surgery, 29(3), 248-251, (2001).

23. Shomali, Z., Kovács, R., Ván, P., Kudinov, I. V., & Ghazanfarian, J., *Lagging heat models in thermodynamics and bioheat transfer: a critical review*. Continuum Mechanics and Thermodynamics, 34(3), 637-679, (2022).

Asif Nawaz,
Department of Physics,
Islamia College Peshawar, KP,
Pakistan.
E-mail address: asifnawaz503@gmail.com

and

Ghulam Saddiq,
Department of Physics,
Islamia College Peshawar, KP,
Pakistan.
E-mail address: dr.saddiq@icp.edu.pk

and

Muhamad Shahid,
Higher Education Department,
KP,
Pakistan.
E-mail address: bluefiber08@icp.edu.pk

and

Ahmad Saeed,
Department of Physics,
Federal Urdu University of Arts, Sciences and Technology, Islamabad,
Pakistan.
E-mail address: ahmad.saeed@fuuast.edu.pk

and

N. A. Mardhiah Zainuddin,
Photonics Research Centre,
Universiti Malaya, 50603 Kuala Lumpur,
Malaysia.
E-mail address: ainaamardhiah92@gmail.com

and

Rozalina Zakaria,
Photonics Research Centre,
Universiti Malaya, 50603 Kuala Lumpur,
Malaysia.
E-mail address: rozalina@um.edu.my